NASA Technical Translation NASA TT F-14,908

THE MARS 2 AND MARS 3 ORBITAL SPACECRAFT: RESULTS OF STUDIES OF THE SURFACE AND ATMOSPHERE OF MARS

V. I. Moroz

Translation of
"Orbital'nyye Apparaty Mars-2 i Mars-3:
Rezul'taty Issledovaniy Poverkhnosti i Atmosfery Marsa,"
Academy of Sciences USSR, Moscow, 1973,
Unpublished Report
18 pages.

N 70K

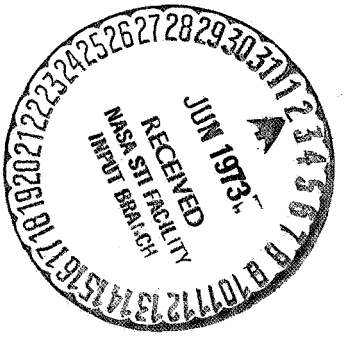

(NASA-TT-F-14908) THE MARS 2 AND MARS 3 ORBITAL SPACECRAFT: RESULTS OF STUDIES OF THE SURFACE AND ATMOSPHERE OF MARS (NASA) 39 p

N73-73332

Unclas
00/99 05809

NATIONAL AERONAUTICS AND SPACE ADMINISTRATION
WASHINGTON, D. C. 20546 APRIL 1973

THE MARS 2 AND MARS 3 ORBITAL SPACECRAFT: RESULTS OF STUDIES OF THE SURFACE AND ATMOSPHERE OF MARS

V. I. Moroz

1. Introduction

/1*

Six different experiments were carried on the Mars 2 and Mars 3 orbital spacecraft to study the physical parameters of the surface and lower atmosphere of the planet:

1) measurement of the surface temperature by radiation in the 8-40 μ band [1, 2, 3];

2) measurement of the soil temperature at a depth of several tens of centimeters and dielectric constant using radiation at 3.4 cm wavelength [4];

3) determination of relative altitudes on the surface of the planet from the intensity of the CO_2 bands around 2 μ [1, 2, 5];

4) photoelectric measurements of surface brightness in six narrow intervals from 3700 to 13,800 A [1, 2, 6, 7];

5) measurement of H_2O content in the atmosphere from the intensity of the absorption band at 1.38 μ [1, 2, 7];

6) radio transmission through the atmosphere, in order to determine the density of neutral gas in the lower atmosphere and the electron density of the ionosphere [8].

The infrared radiometer and photoelectric photometers at the CO_2 and H_2O bands and the sectors of the continuous spectrum selected were briefly described earlier in [1, 2, 5, 6, 7, 9], the parameters of the radio telescope were presented in [4]. Table 1 presents a summary of the main characteristics of all the devices (field of vision, accuracy of measurements). The optical axes of all devices were parallel and the parameters of the surface and atmosphere were measured over the same areas of the planet. The brightness in the various wavelength ranges,

/2

*Numbers in the margin indicate pagination in the foreign text.

surface and soil temperature, dielectric constant, altitude, pressure and H_2O content in the atmsophere were determined for the same sectors.

The instruments are rigidly connected to the body of the spacecraft and their orientation in a constant direction during measurements was usually assured by the sun-star orientation system of the spacecraft. As the pericenter of the orbit was approached, the instruments were turned on for several minutes before intersection of the limb by a special optical sensor. The optical axes intersected the planet generally on a line close to a great circle and the passage from limb to limb required about 30 minutes. Subsequently, we will refer to the track of the optical axis on the surface of the planet as the measurement track. According to our preliminary estimates, the accuracy of determination of the measurement track is 1-2° according to the areographic coordinates.

In the experiments [1-5], all the results produced relate to Mars 3. Its period of revolution is about 12 days. Figure 1 shows seven measurement tracks made by this spacecraft.

The distance at the pericenter to the surface of Mars changes slightly with evolution of the orbit and varied during this period from approximately 1000 to 15,000 km. The first three passages, 15 December 1971, 27 December 1971 and 9 January 1972, occurred during a dust storm and as the dust storm quieted, while the remaining passages occurred after the end of the dust storm. In December, January and February, the measurement tracks corresponding to the successive dates of passage of the periares were shifted relative to each other by approximately 90° of longitude. As a result, significant sectors of the tracks of 3 February 1972, 16 February 1972 and 28 February 1972 passed close to the tracks of 15 December 1971, 27 December 1971 and 9 January 1972, and we have measurements for the same areas of Mars produced during a storm (more precisely during its last

stages) and after a storm. The track of 12 March 1972, for a number of reasons, has not yet been correlated to the surface sufficiently reliably and its position, shown on Figure 1, must be considered approximate.

In general, the volume of information produced by Mars 3 /3 is significantly less than by Mariner 9. However, Mars 3 included experiments which were not carried on Mariner 9 at all (photoelectric photometry in the near infrared and visible areas of the spectrum, radio astronomical measurements), and as concerns the experiments similar to those carried by Mariner 9 (IR radiometry, optical altimetry, measurement of H_2O content), the results of Mars 3 are of interest not only as supplementary material but also since they allow combined analysis of the area with the photometric and radio astronomical data and were performed using methods which were significantly different.

In particular, the measurements of the content of H_2O and CO_2 altimetry in our experiments were performed in bands in the near infrared area, and the results of the measurements were practically independent of the vertical temperature distribution. On Mariner, the same data were produced using bands in the far infrared area of the spectrum, which depends so strongly on the vertical temperature profile that it can be observed in emission and in absorption [10]. Although analysis of the spectra produced by IRIS does yield the vertical temperature profile at the same time, the task is significantly complicated and, probably, does not always allow unambiguous solution. The topographic material produced on Mariner 9 by ultraviolet photometry [11] is highly valuable due to its global coverage, but must be approached with caution, since it is strongly influenced by heterogeneities in the dust content of the atmosphere.

In the following, we will attempt to present a brief review of published data as well as our new results. They refer to the first six sessions of Mars 3.

We are grateful to N. N. Krupenio and I. B. Drozdovskaya, who provided us with the results of the radio astronomy experiment before their publication.

We are also grateful to D. Sneiderman (NASA) for providing us with the Mariner photographs of the surface of Mars in areas along the measurement tracks of Mars 3. In many cases, they helped our interpretation of our measurements. Comparison of these photographs with the photometric curves confirmed that the tracks were defined with the accuracy of 1-2° indicated above, and the position of the tracks may be refined still further in the future using the Mariner photographs.

/4

2. Direct Results of Measurement

Figures 2-7 show the results of measurements for six tracks relating primarily to the surface. The infrared brightness temperature T_B, soil temperature T_{ss} (at a depth of a few decimeters) measured by means of radiation at 3.4 cm, dielectric constant ε, brightness in the continuous spectrum (photometric profile) in the near infrared (1.4 μ), altitude Z relative to the 6 mb level are presented. Here for comparison with the measurement results we also present the values of μ_1 -- the cosine of the zenith distance to the sun and $\overline{T}_s$ -- the theoretical mean daily temperature of the surface.

Figure 8 shows separately the altitudes for 27 December 1971. They are separated due to the fact that they clearly relate not to the surface but rather to the cloud cover over a significant portion of the track.

Figures 9-14 show results relating primarily to the atmosphere: pressure P, profile of H_2O content, brightness (photometric profile) in the near ultraviolet at 3700 A. Here also we show the brightness at wavelength 4940 A, which is determined by scattering both by the surface and by the atmosphere and at 6940 A, which is determined primarily by the surface (as is the

brightness at 1.4 μ). This comment is accurate only for measurements performed after the end of the dust storm. On the tracks of 15 December 1971 and 27 December 1971, the brightness in both the red and near infrared areas result to a significant extent from reflection by the dust clouds.

The method of processing of the infrared temperatures was described in [1-3]. Let us recall that our radiometer utilized /5
a wide filter and in the area of the fundamental absorption band of CO_2 (? 15 μ), the radiation was determined by the atmosphere, which, depending on specific conditions, may be colder or warmer than the surface. In order to consider the influence of the atmosphere in the very first approximation in the 15 μ band, we increased the fluxes measured by 50 (which yields a temperature correction of about 1%). Actually, the magnitude and sign of this correction depend on the local time, model of the atmosphere and zenith angle of the apparatus. For the future, we suggest that the correction for absorption be defined more precisely.

The infrared brightness temperature T_B is quite similar to the kinetic temperature of the surface layer T_s. Actually, ignoring the difference between T_t and the effective temperature T_e, we have

$$T_B^4 = b_1 T_s^4 \qquad (1)$$

where b_1 is the radiation factor in the infrared band. Laboratory measurements [12] for terrestrial materials yield $b_1 \simeq 0.95$, so that if we assume the same value for Mars, the difference of T_B and T_e from T_s will be on the order of 1%. The ratio T_b/T_s depends on b_1 quite weakly, as the fourth root. The situation is worse in the radio band, where the relationship

$$T_B = b_2 T_{ss} \qquad (2)$$

applies. Here the error due to uncertainty in the value of b_2 (radiation factor in the radio wave band) is somewhat greater. However, the radio experiment was constructed (measurement of two polarizations) such that it allowed b_2 and T_B to be determined separately. In processing the observations, it was assumed that the surface of Mars can be represented as a smooth sphere. The radiation factor for the sum of the two polarizations in this case is, according to Fresnel's law,

$$b_2 = 1 - (dg^2(z' - z))/(dg^2(z' + z)) - \\ - (\sin^2(z' - z))/(\sin^2(z' + z)) \qquad (3)$$

where z is the zenith angle of the apparatus, z' is defined by the /6 relationship

$$\sin z/\sin z' = h - \sqrt{\varepsilon} \qquad (4)$$

Figures 2-7 show the values of T_{ss} and ε separately. The errors in determination apparently result from variations between the actual surface and the hypothesis assumed of the surface as a smooth sphere. Values too high and too low lead to increased and decreased values of T_{ss} respectively. These points can be discarded if we compare T_{ss} with the mean daily surface temperature $\overline{T}_s$. For Martian soil we must expect that these quantities should be similar. We have entered on Figures 2-7 the values of $\overline{T}_s$ as calculated by the formula

$$\overline{T}_s = \left(\frac{E_0}{\sigma r^2} \frac{1 - A}{b_1} \frac{}{\overline{\cos z}}\right)^{1/4} \qquad (5)$$

where $\overline{\cos z}$ are the mean daily values of the cosine of the zenith angle of the sun, A is the integral albedo, E_0 is the solar

constant, r is the distance to the sun in astronomical units. We assumed that $1 - A/b_4 = 1$. On the average, the values of T_{ss} fall below the curve of $\overline{T}_s$ by approximately 20°, which can be explained by inaccuracy of calibration.

The method of determination of pressures and relative altitudes was described in [1, 2, 5], the method of determining content of water vapor in [7].

Only relative measurements of brightness B were performed, but it is significant here that the scale of brightnesses is the same for all sessions. The absolute brightness units, laid out on the ordinates for 1.38 μ, were produced on the assumption that in the sessions of 16 February 1972 and 28 February 1972 the brightness in the light areas follows the rule of Lambert and the brightness factor (visible albedo) for the light areas is 0.41.

The fact that a dust storm was in process on Mars during the time when the measurements began has both negative and positive aspects. The negative aspect is obvious: the presence of the dust clouds hindered photography of the surface and reduced the possi- /7
bility of a number of optical experiments (H_2O and CO_2 photometry) during the first two sessions. However, the dust storm was also useful, since such broad capabilities had never before been provided for the study of the nature of this powerful and curious phenomenon.

3. When Did the Dust Storm End and How Much Did it Influence the Results of Measurement?

Acceptable television images were produced by the Mariner spacecraft quite regularly beginning in late December; however, to the extent that can be judged from the photographs available to us, the transparency of the Martian atmosphere continued to increase during this time.

The change in transparency with time can be traced on our photometric profiles. Table 2 presents the sea/continent

contrasts for 1.38 μ during various sessions. Here also we show the cosines of the zenith angles of the sun and the apparatus (μ_1 and μ_2), and phase angles α. The contrasts are the ratio $(B_c - B_m)/B_c$, where B_m is the brightness of the maria (solid curve), B_c is the brightness of the continents (dotted curve), yielding the Lambert interpolation of the brightness level corresponding to the continent. Table 2 also presents the values of brightness factor R_{max} corresponding to the dotted curve for each /8 track. Obviously, in general they decrease systematically, 15 December showing R_{max} 15% greater than in the next two sessions in February.

TABLE 2

Session	$(B_c - B_m)/B_c$	φ	λ	μ_1	μ_2	α	R_{max}
15.12.71	0.25 M. Cimmerium	-30	222	0.457	0.976	52	0.47
27.12.71	0.32 Lapigia	-26	304	0.535	0.992	53	0.45
09.01.72	0.51 M. Ergthraeum	-23	29	0.606	0.999	54	0.44
03.02.72	0.39 M. Cimmerium	-30	215	0.826	0.855	56	0.45
16.02.72	0.56 Lapigia	-25	299	0.872	0.816	57	0.41
28.02.72	0.55 M. Ergthraeum	025	30	0.671	0.915	59	0.41

On 9 January 1972, the mare/continent contrasts were similar to the values achieved in the February sessions, although there still is some difference.

The transparency of the atmosphere obviously depends on latitude. At latitudes south of 50° in sessions on 15 and 27 December the B(1.38) profile contains a larger quantity of fine details, whereas near the equator there are no such fine details, the maria showing as smooth minima. On 15 December, the red profile (6940 A) shows Prometer Sinus, but Mare Cimmerium is not visible at all.

The general impression is that on 15 and 27 December 1971, the dust content of the atmosphere was so high that the results of measurement of pressure and altitude and H_2O content for

latitudes north of 40° are strongly distorted by the dust storm. The similar results for 9 January 1972 still contain some uncertainty. Therefore, the pressures, altitudes and H_2O contents for the first sessions are illustrated by dotted lines, and these curves are not presented at all for 27 December 1972, since the equivalent widths of the CO_2 bands were very slight on this session. A separate figure (Figure 8) shows the altitudes for this session, which were subsequently used to determine the altitudes of the upper boundary of the clouds.

The altitudes determined in the sessions of 15 December 1971 and 9 January 1972 can probably be used with caution as qualitative characteristics of the relief.

The infrared temperature, determined from the radiation in the 8-40 μ band, even for the December sessions, relates to the surface. Two factors indicate this:

1) The transparency of the atmosphere clearly increases with wavelength upon transition from 0.7 to 1.4 μ. If this is explained by the small dimsensions of the particles, which is most probable, for radiation with $\lambda > 8$ μ, the dust clouds should be fully transparent. /9

2) The dependence of temperature on local time agrees rather well with the theoretical dependence calculated without considering radiation of the atmosphere. The difference is only that the measured temperature curve is somewhat lower than the theoretical curve, which is explained by the absorption of solar radiation in the dust clouds [1, 2, 3, 6]. This means that the optical thickness of the dust clouds in the $\lambda > 8$ μ area is slight.

4. Surface of Mars: Temperature, Soil Density, Altitude.

Temperature and Thermal Properties of the Surface Layer

The theoretical effective temperatures of the surface T_e were calculated for various values of thermal inertia constant $(k\rho e)^{1/2}$. For values of integral albedo A = 0.25 (light areas) and A = 0.15

(dark areas). The profiles of T_B for 16 February and 28 February 1972 are satisfactority approximated by the theoretical curves with $(k\rho e)^{1/2} = 0.006$ cal cm^{-2} $sec^{-1/2}$ deg^{-1} (Figures 15 and 16). The exceptions are the latitudes $\phi > +40°$, where the measured temperatures are much lower than the theoretical temperatures, near the condensation point of CO_2 at latitudes $\phi \geq +50°$.

An elevated value of thermal inertia factor (0.008) occurs in the region of the compact dark area Cerberus. The precise correlation between T_B and brightness B (1.38) is obvious. Areas with lower brightness (lower reflective capacity) have higher temperatures.

During the dust storm (15 and 27 December 1971), the surface temperature was lower than the "normal" temperature [1, 2, 3, 6]; this is also indicated by the Mariner measurements [13] and terrestrial observations by the author and his colleagues [14].

Temperature, Dielectric Constant and Density of Soil (Results of Radio Astronomy Experiment)

The soil temperature at a depth of a few decimeters agrees satisfactorily with the calculated mean daily temperatures. As would be expected, there are no indications of daily fluctuations in soil temperature. If we discard the sectors where the temperature T_{ss} differs sharply from the calculated $\overline{T}_s$, the mean value of dielectric constant /10

$$\varepsilon' = 4 \pm 1,$$

which corresponds to the normal (z = 0) radiation factor $\varepsilon = 0.9$.

The dielectric constant for most dehydrated terrestrial minerals, as Krotikov has shown [15], is related to soil density ρ by the relationship

$$\rho = 2(\sqrt{\varepsilon} - 1) \text{ g cm}^{-2}, \quad (6)$$

from which for the density of the Martian soil we have the estimate

$$\rho = 2 \text{ g cm}^{-2}.$$

Comparing B (1.38 μ) and ε on the tracks of 9 January 1972 through 28 February 1972, we can see that in the dark areas there is a tendency toward higher ε (and, consequently, density).

Altitudes

The altitude profiles also correlate with brightness, though to a lesser extent than the infrared temperatures, but there is doubtless a correlation. This correlation is not always precise and in the first publications [1, 2, 5], no attention was turned to it. Comparing the altitude profiles and brightness profiles, on Figures 2-7 we can nevertheless see that the darker regions are most frequently higher than neighboring lighter regions.

The altitudes relative to the 6 mb level on our tracks fall between - 1.5 and 6 km. The highest areas are located in Mare Australis (track of 9 January 1972, 5-6 km), [illegible] (track of 16 February 1972, about 4 km), [illegible] (track of 28 February 1972, about 4 km), while the lowest are in [illegible] (track of 16 February 1972, about -1 km), Chrise [?] (track of 28 February 1972). The tracks of 16 and 28 February 1972, reaching far into the northern latitudes, show a tendency toward systematic reduction in altitude in the northern hemisphere. This is also indicated by the radio occultation experiments of Mariner [15].

5. The Atmosphere of Mars: Pressure, Water Vapor, Dust Storm, High-Latitude Clouds /11

Pressure

The absolute values of pressure determined from our observations are insufficiently reliable for final conclusion; however,

the impression is created that the 6 mb value is somewhat higher than the mean actual value. It is apparently closer to 5-5.5 mb. The pressures measured over all tracks vary from 3.5 to 7 mb.

Radio occultation observations of Mars 2 yield pressures of 5-10 mb [8]; these results will apparently be refined.

Water Vapor

On the tracks of 16 February 1972 and 28 February 1972, the content of water vapor in the atmosphere reached U_0 = 6-8 μ precipitated water. Mariner 9 [12] and terrestrial observations performed at the same time [16] yield about 10 μ precipitated water as an average for Mars. The agreement can be considered satisfactory, considering the possibility of geographic and time fluctuations (as well as variations in our calibration). The increase in U_0 during the period from December through February, recorded by measurements on Mars 3, was independently confirmed by terrestrial observations [16]. There is some correlation between the water content in the vertical column and the pressure, as would be expected with no saturation (relative humidity on the order of a few percent) everywhere except in the cold areas of the northern hemisphere. The sharp decrease in moisture in the latitudes north of +50° is accompanied by the formation of the polar area clouds, which strongly scatter UV radiation (see Figure 13). On the average, the content of water vapor in the atmosphere of Mars during the measurements was several times less than during the same season indicated by terrestrial observations during previous oppositions.

Dust Storm

We will touch upon three questions -- the altitude of the clouds, dimensions of particles and the influence of the dust storm on the thermal mode on the surface. /12

a) Altitude of Clouds

On the track of 27 December 1971 (in the area to the north of -30°), processing of the observations of the CO_2 photometer using the standard method showed very low values of pressure (as little as 2 mb) and altitude (up to 10-15 km). It was natural to assume that these pressures and altitudes relate to some effective reflecting level in the clouds. Thus, their altitude is on the order of the altitude of the homogeneous atmosphere of the planet. Similar results were produced by terrestrial observations made by the author and O. G. Taranova [17], as well as Parkinson and Hunten [18]. The distribution of temperature with altitude produced in the two Mariner experiments (IRIS, see [10], and the radio occultation measurements [15]), independently indicated great altitude of the clouds.

b) Estimate of Dimensions of Particles

We will discuss this problem in somewhat greater detail, since there is a contradiction here between various authors. Moroz et al. [1, 2 7] give the estimate

$$\gamma \simeq 1\ \mu.$$

A similar value is reported by Pang and Hold [19]

$$\gamma \simeq 2\ \mu.$$

A considerably larger radius is given by Leovy et al. [20]

$$\gamma \simeq 10\ \mu.$$

All three estimates are based on photometric arguments. Of course, dust clouds are heterogeneous in different areas and particles of different dimensions may be present at different altitudes. However, the method used by the authors of [20] is

objectionable in principle. Their arguments can be reduced to the following:

1) The albedo of the clouds in the visible area of the spectrum is slight ($\simeq 0.13$); therefore, the albedo of single reflection is slight. The albedo of single reflection is less, the greater the dimensions of the particles. Without presenting /13 calculations, the authors of [20] state that the observed albedo can be achieved only with dimensions of several tens of microns.

2) There are photometric and radiometric arguments indicating that the surface layer consists of grains measuring several tens of microns. The authors of [20] consider it natural to expect that the dust clouds would consist of particles of the same size.

Neither argument seems convincing to us. The same particles have much greater one-time scattering albedo in the red and near infrared areas of the spectrum, and obviously the grains of the surface layer might be much greater than the mean diameter of particles suspended in the atmosphere.

Our estimate is based on the simple fact that the transparency of the clouds at 1.4 μ wavelength is significantly greater than at 0.7 μ. This can be particularly clearly seen from comparison of the red (0.694 μ) and infrared (1.38 μ) profiles of 15 December 1971. Since the albedo of the clouds (and consequently their true absorption) at these wavelengths is practically identical, the difference in transparency can be explained only by the rather small ratio of radius to wavelength. An approximate quantitative analysis gives us the estimate presented above of $\gamma \simeq 1$ μ.

The optical thickness

$$\tau = \int_0^\infty \alpha_z dz$$

(where α_z is the extinction factor) to explain the observations of 15 December 1971 at this radius should be about 3 for 1.4 μ and over 6 for 0.7 μ.

An accurate mean estimate of the particle diameter is very important for the entire concept of the dust storm. If the particle diameter is on the order of 1 μ, they could be suspended in the atmosphere on the order of 100 days, and long-term support of dust clouds would not require strong vertical movement in the atmosphere. In this case, the dust storm is a storm in the direct sense of the word only in its initial stage, after which the wind /14
speed decreases and the second phase, the phase of slow settling, begins.

If, however, the estimate of Leovy and his colleagues is correct, and the particles are larger, the settling time would be but a few days and strong atmospheric movement would be required throughout the entire period over which the dust clouds were observed in order to support the clouds.

The optical thickness $\tau \simeq 3$, $\gamma \simeq 10^{-4}$ cm with density $\rho \simeq 3$ g cm^{-2} yields a dust mass in a column with a cross section of 1 cm^2 of about 10^{-3} g cm^{-2}, corresponding to a dust mass of 10^3 tons in the atmosphere of the entire planet.

c) Influence of Dust Storm on the Thermal Mode of the Planet

As was indicated, the temperature of the surface drops during the time of a dust storm. This is a result of the higher transparency of the dust clouds for outgoing longwave radiation of the planet than for shortwave solar radiation. It is natural to refer to this phenomenon as the anti-greenhouse effect, since it is opposite in sign to the greenhouse effect. Semiquantitative analysis of the heat balance of the planet with the anti-greenhouse effect was performed in the work of Ginzburg [21].

High-Latitude Clouds

On the tracks of 16 February 1972 and 28 February 1972, the ultraviolet profiles show a sharp increase in brightness as latitudes of about 35-40° are crossed. The Mariner photographs produced in the same areas a few days later show bright clouds here. These clouds are practically not seen in the near infrared area of the spectrum, which indicates the following:

1) particle dimensions were small (some tenths of a micron);

2) the clouds are fully transparent for surface radiation in the far infrared area, so that the temperature measured here is that of the surface.

Although the surface temperature in this area is near the condensation point of CO_2, the high-latitude clouds do not necessarily consist of solid carbon dioxide, since a temperature inversion may occur here. From the H_2O profiles, we see that water vapor disappears here. The 5-10 microns of precipitated water in the form of small-radius ice particles could provide optical thickness $\tau > 1$, as seen in the shortwave portion of the spectrum. /15

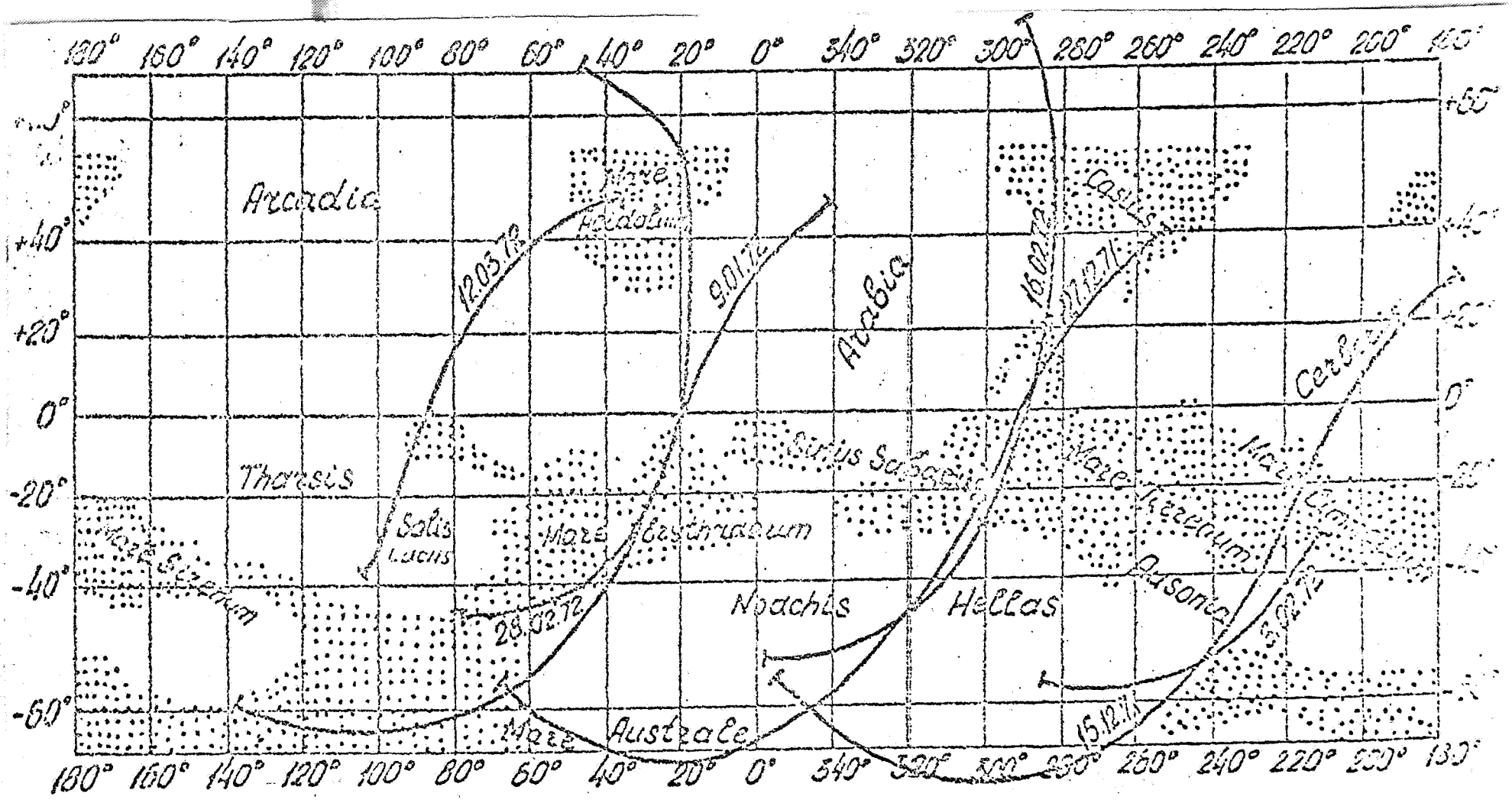

Figure 1. Measurement Tracks of Mars 3

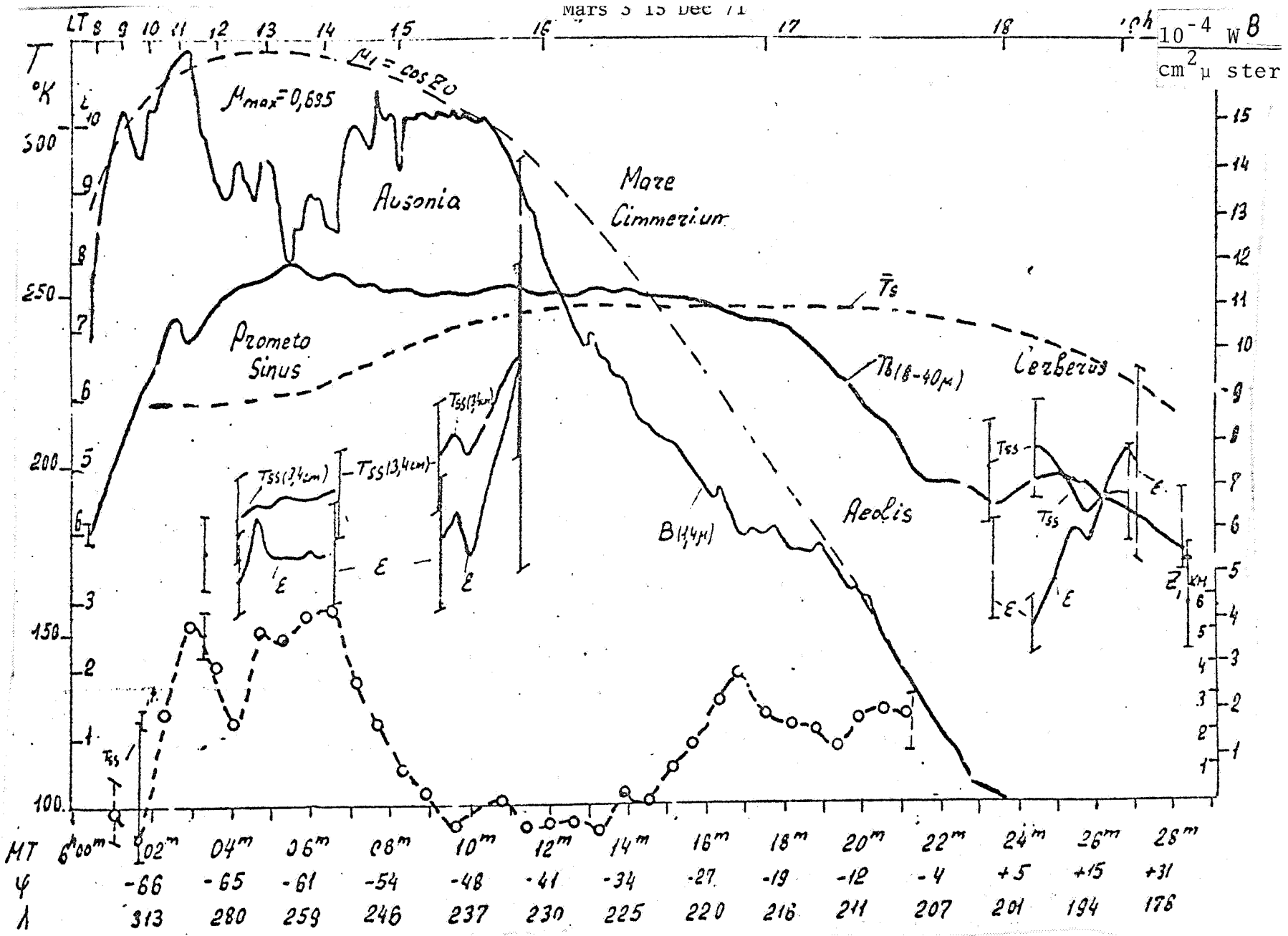

Figure 2. Results of Measurement Along the Track of 15 December 1971. Infrared Brightness Temperature T_e, Soil Temperautre (calculated from Radio Radiation) T_{ss}, Brightness B (1.4 μ) in Continuous Spectrum Around 1.4 μ, Dielectric Constant of Soil ε, Altitude z Relative to 6 mb level. T_e is Calculated Average Daily Temperature, μ_1 is the Cosine of the Zenith Distance of the Sun.

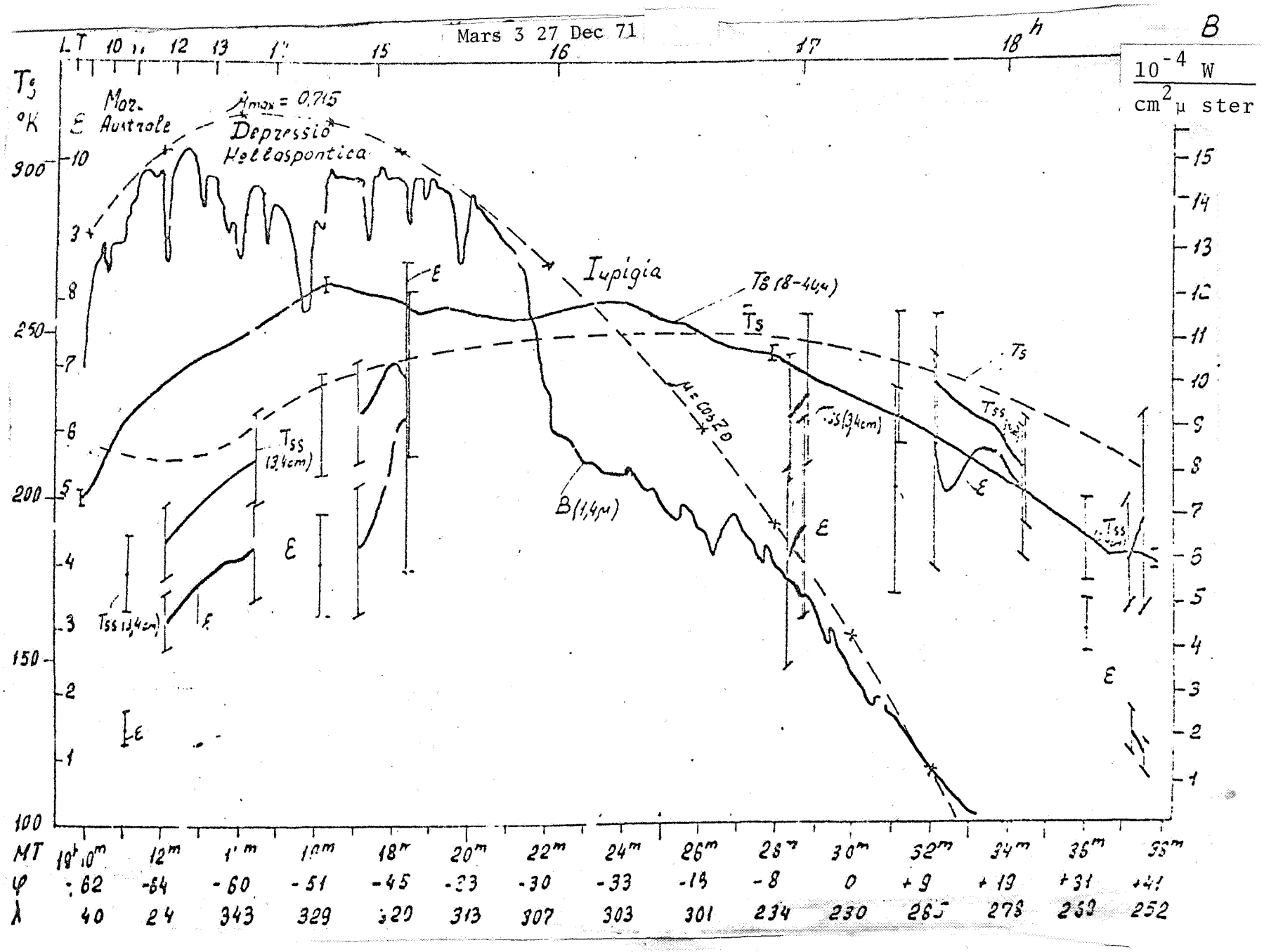

Figure 3. Results of Measurement Along Track of 27 December 1971. Symbols Same as Figure 2.

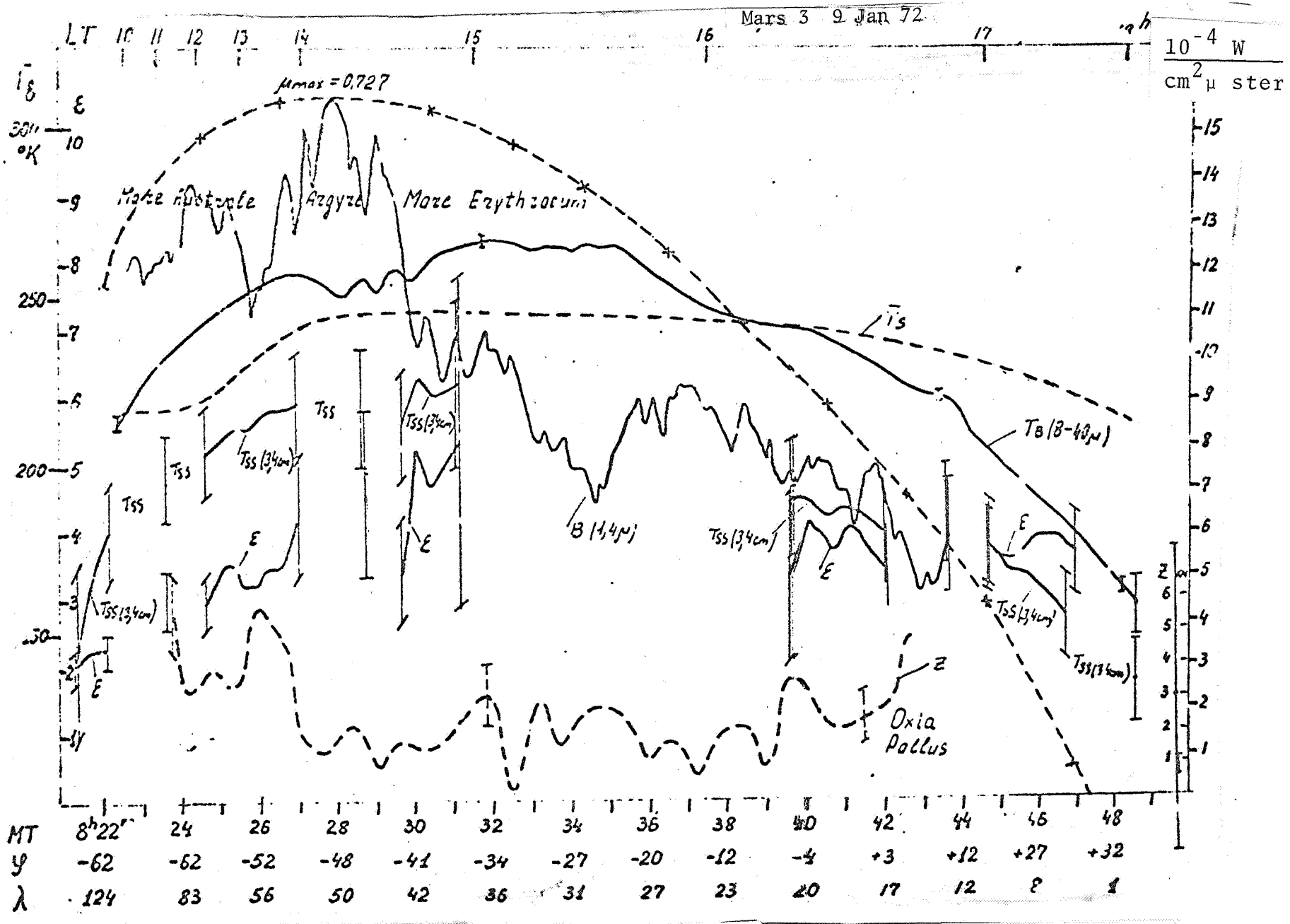

Figure 4. Results of Measurement Along Track of 9 January 1972. Symbols Same as Figure 2.

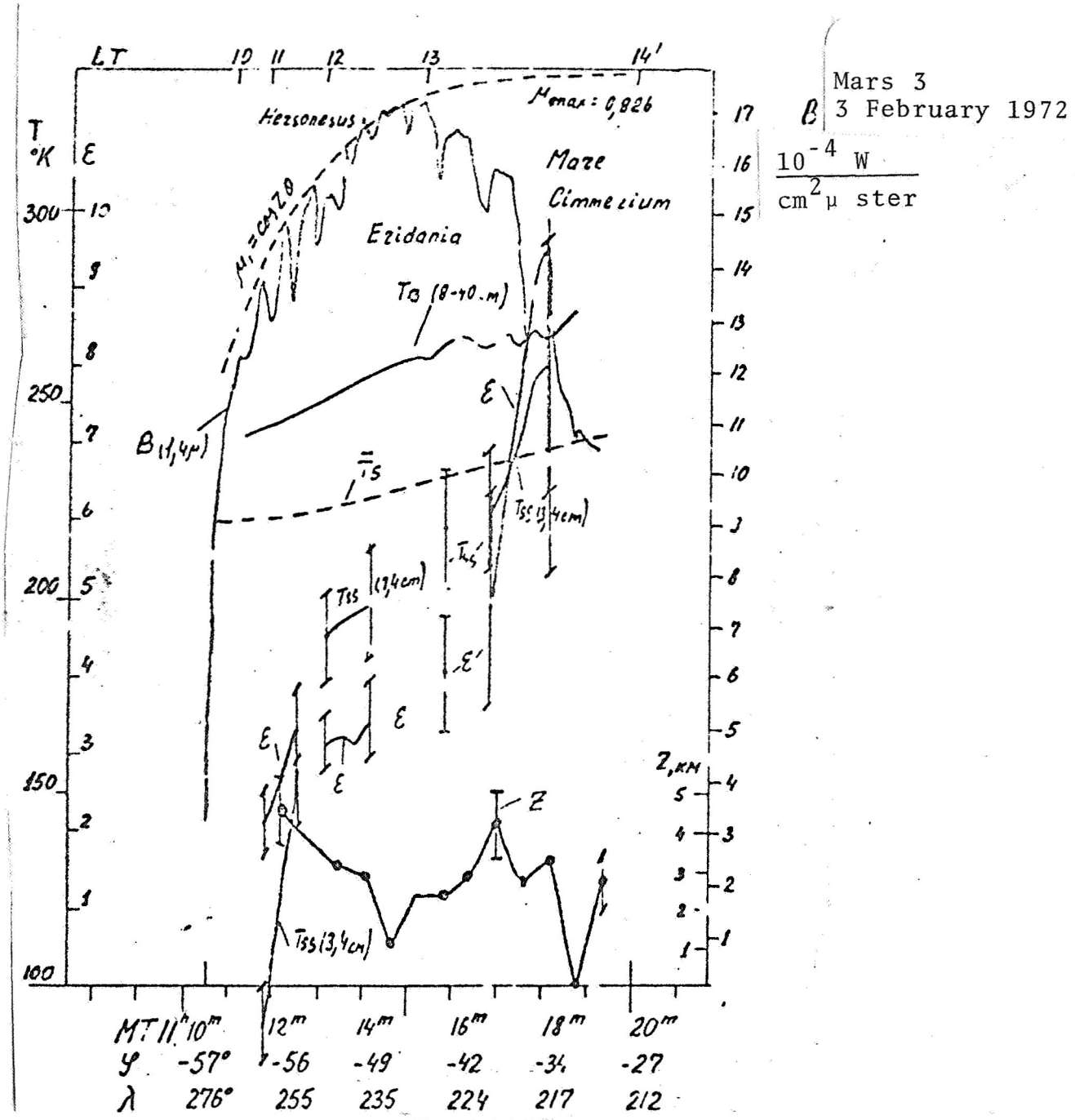

Figure 5. Results of Measurement Along Track of 3 February 1972. Symbols Same as Figure 2.

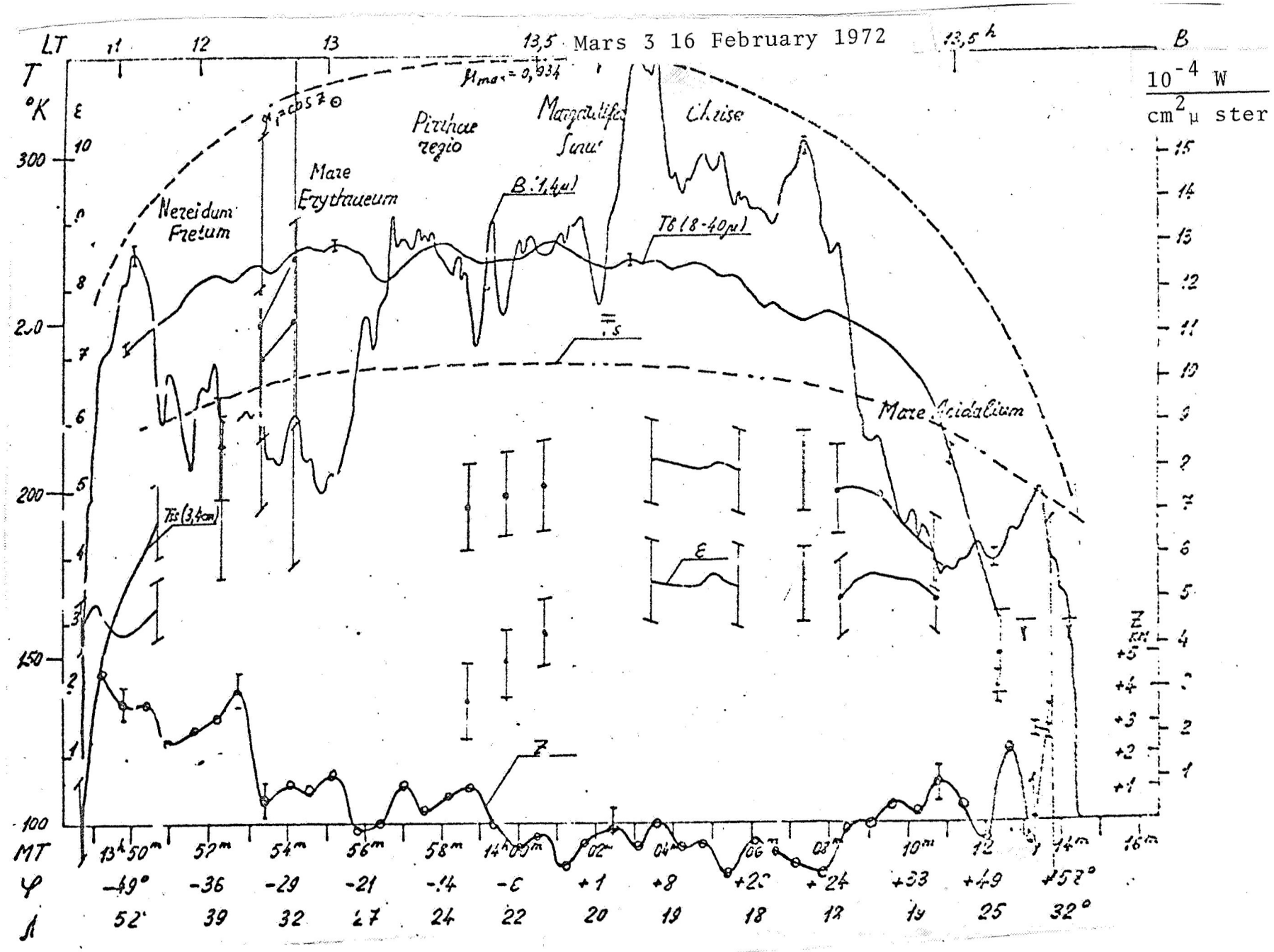

Figure 6. Results of Measurement Along Track of 28 February 1972. Symbols Same as Figure 2.

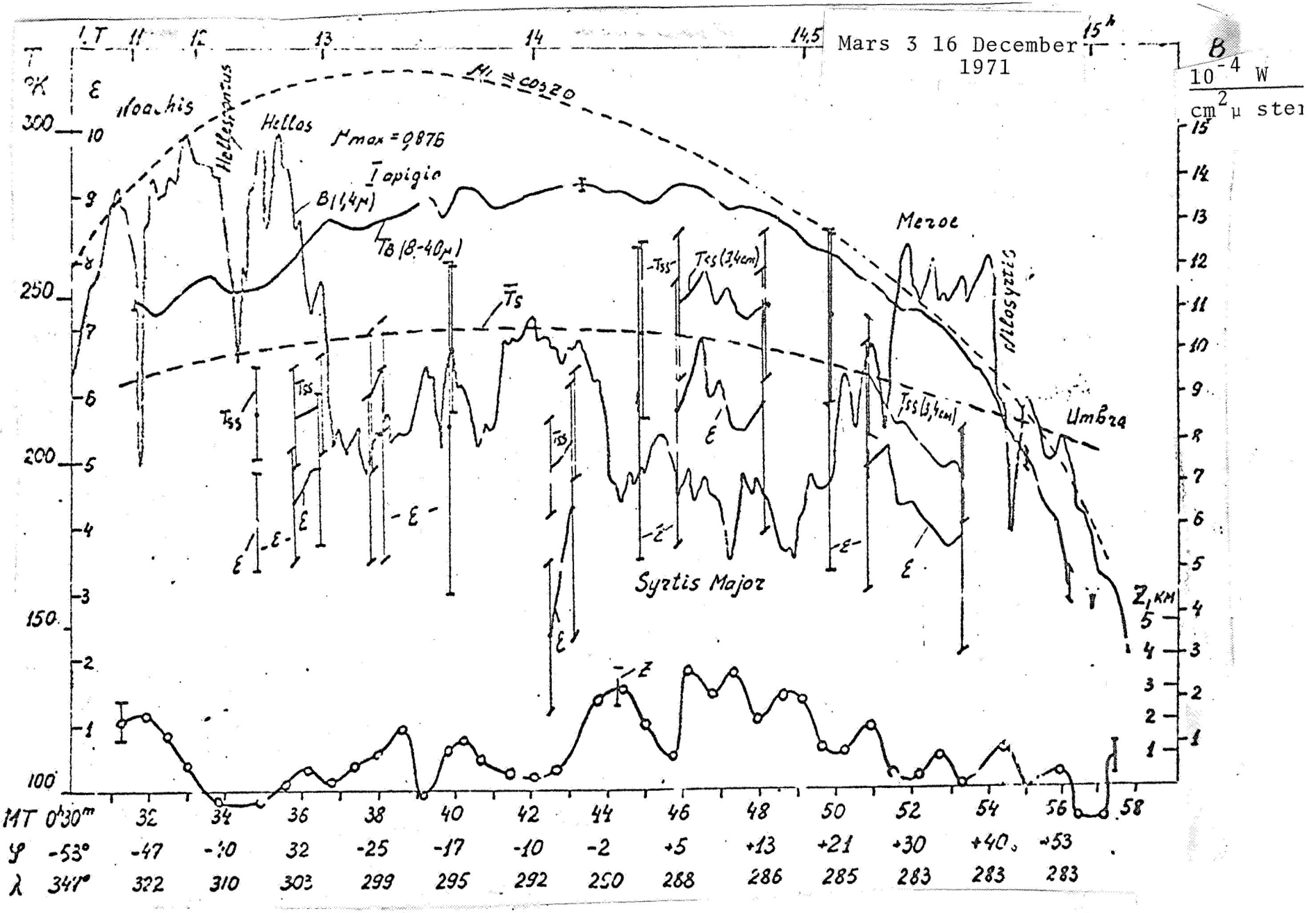

Figure 7. Results of Measurement Along Track of 6 February 1972. Symbols Same as Figure 2.

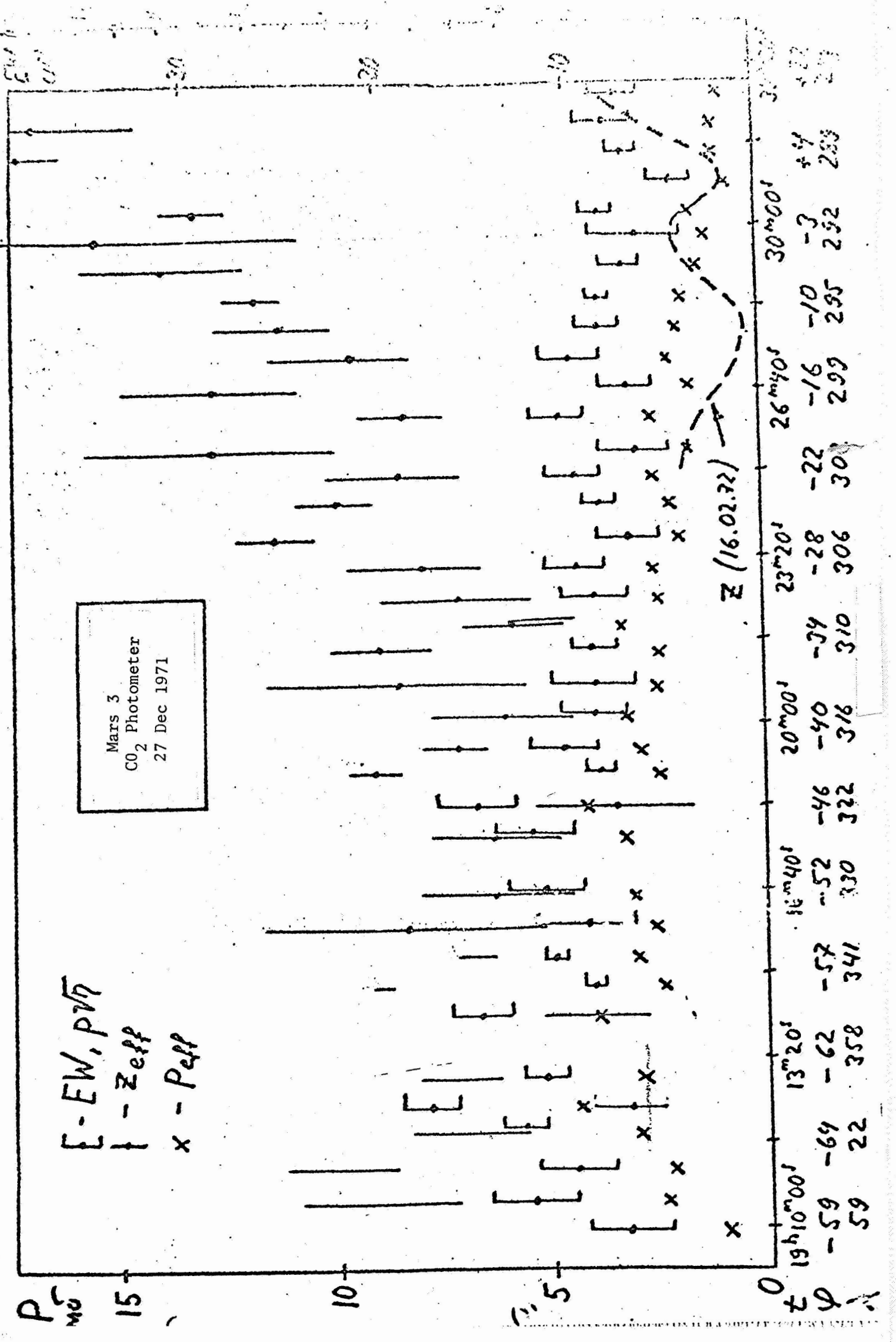

Figure 8. Altitudes According to Measurements of 27 December. In the Right Portion, the Altitude Doubtless Relates to the Upper Boundary of the Clouds, not to the Surface. The Dotted Line Shows the Altitudes for the Corresponding Sectors of the Track of 16 February 1972

Figure 9. Results of Measurements along Track of 15 December 1971. H_2O Content, Pressure, Brightness in Wavelengths 6940, 4940 and 3700 A, μ_1 is the Cosine of the Zenith Distance of the Sun, μ_2 is the Cosine of the Zenith Distance of the Spacecraft.

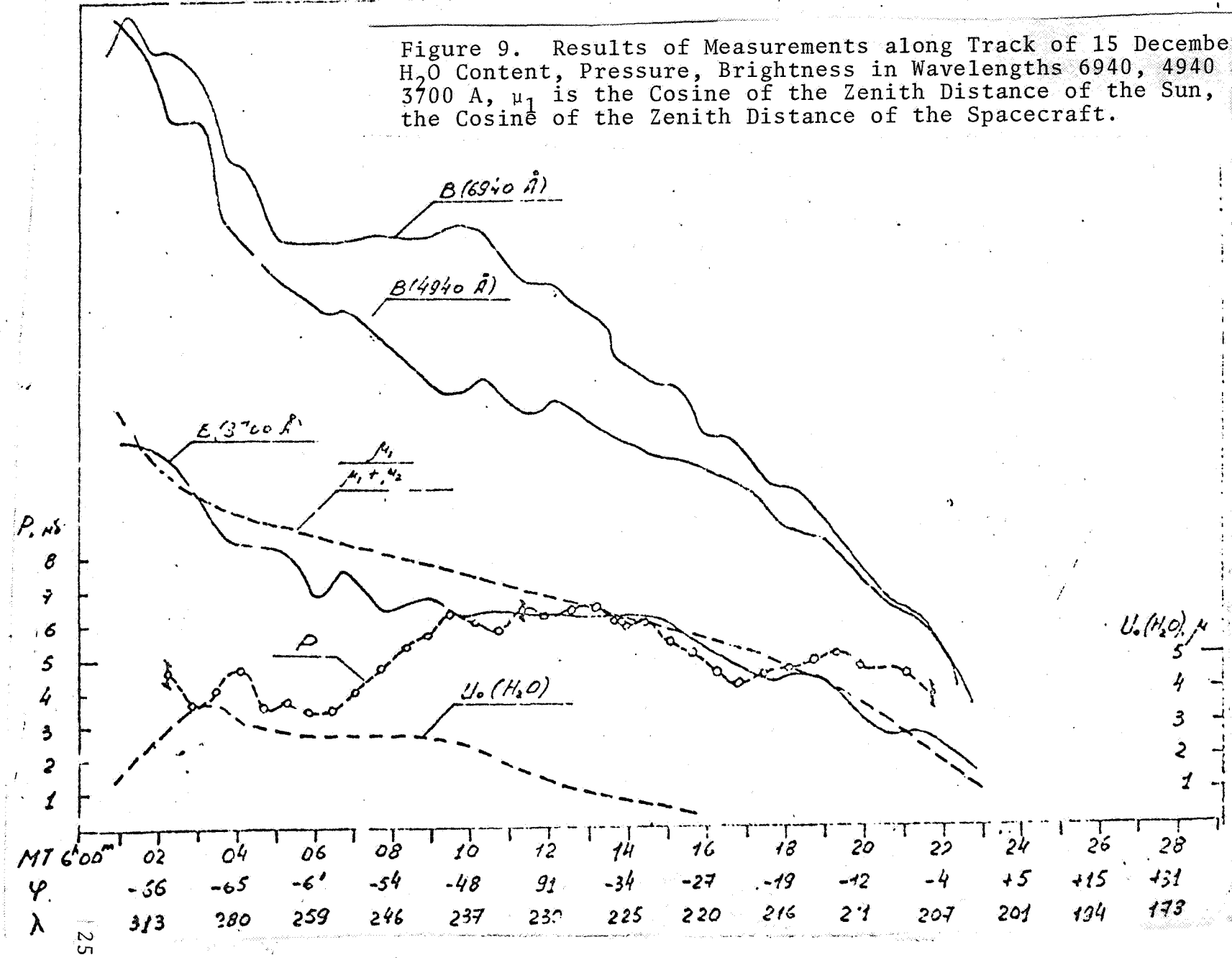

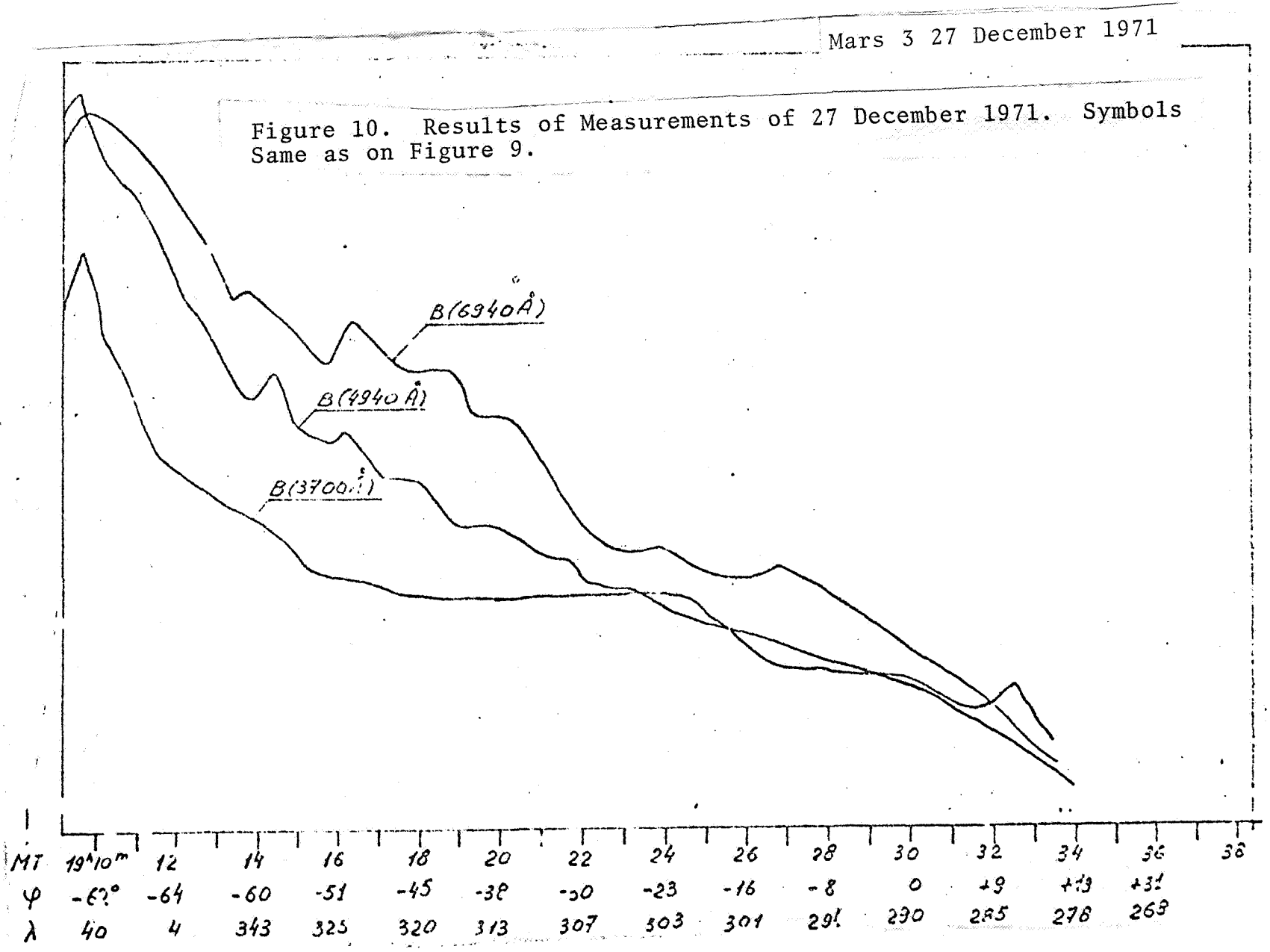

Figure 10. Results of Measurements of 27 December 1971. Symbols Same as on Figure 9.

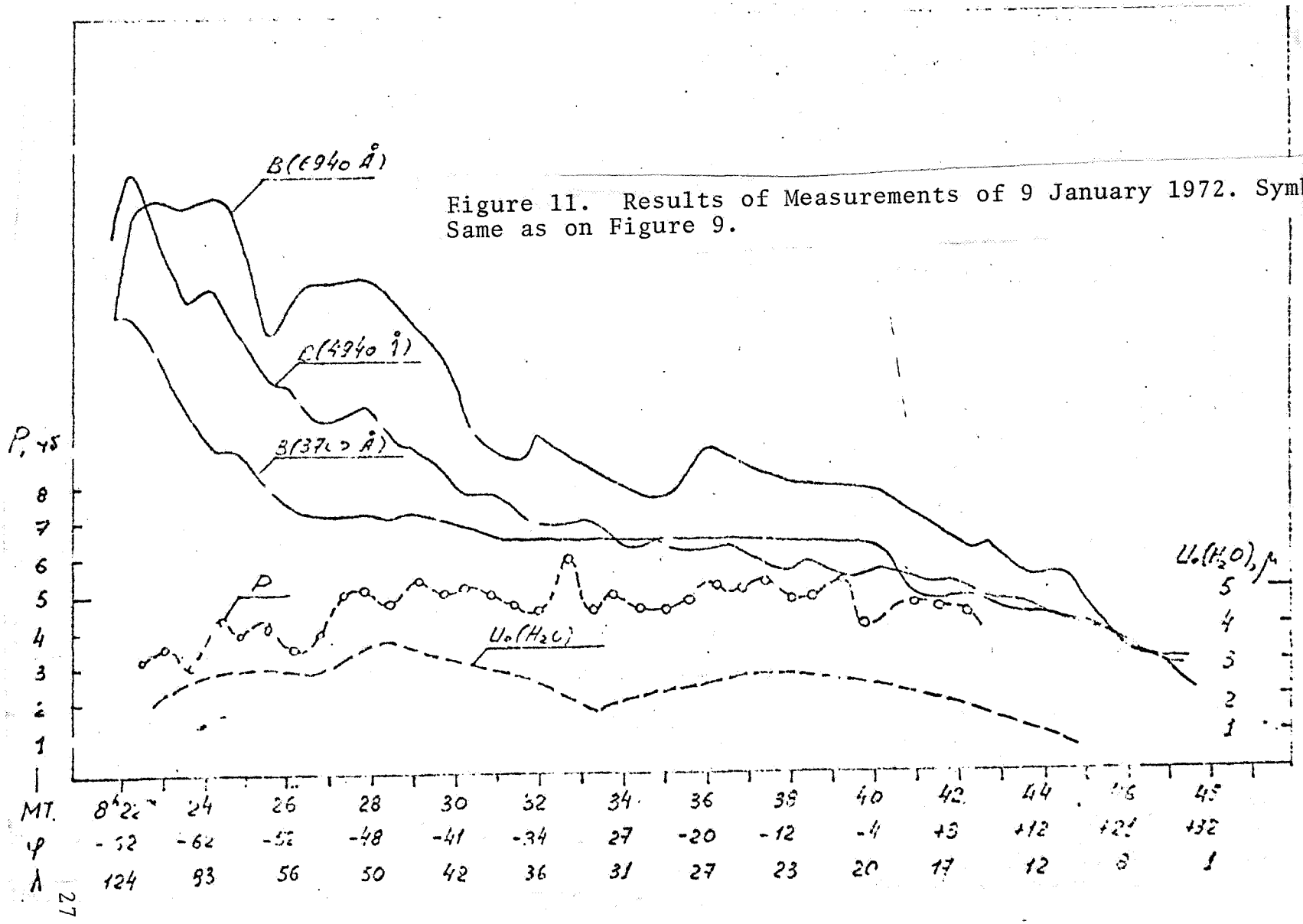

Figure 11. Results of Measurements of 9 January 1972. Symbols Same as on Figure 9.

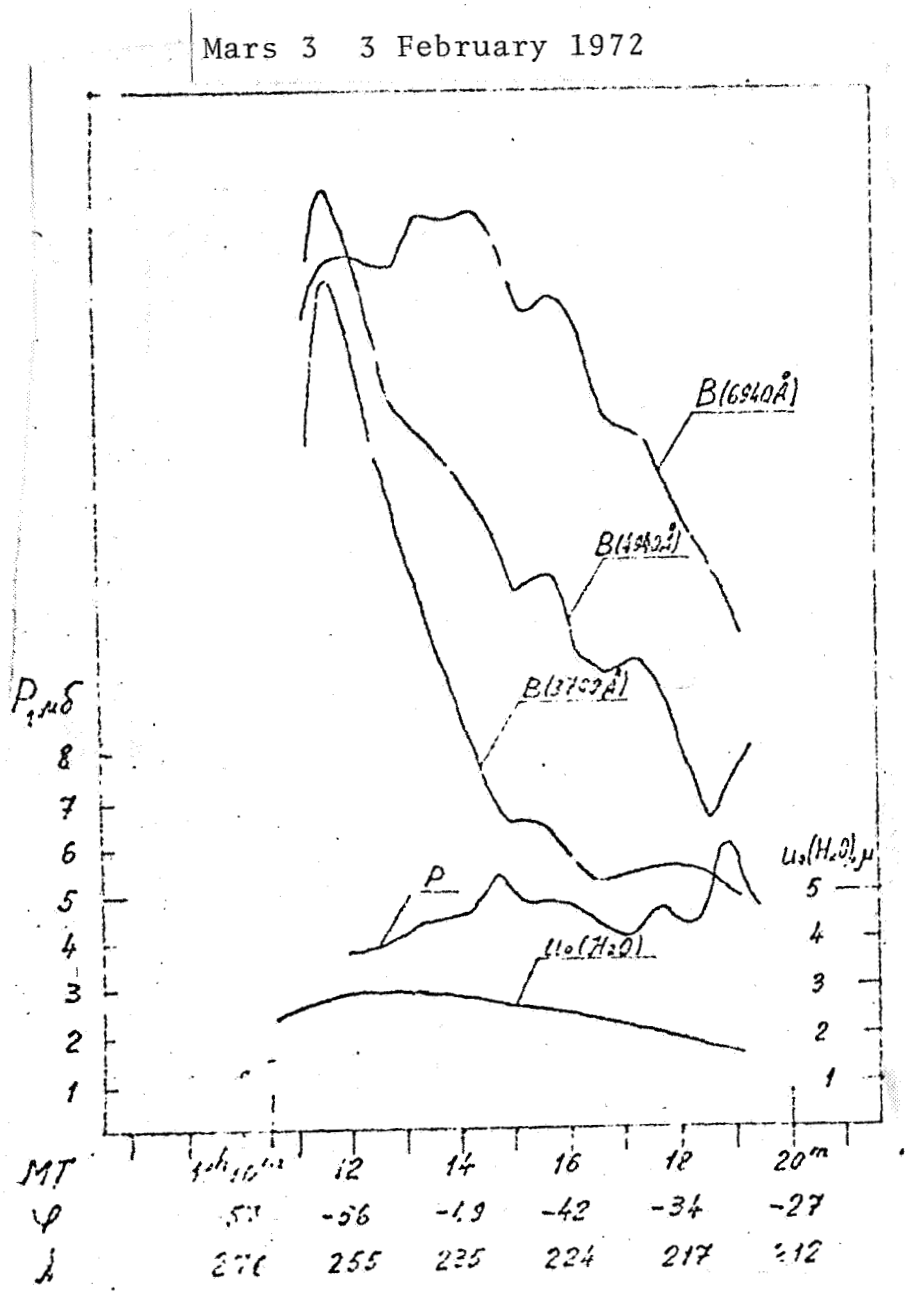

Figure 12. Results of Measurements of 3 February 1972. Symbols Same as on Figure 9.

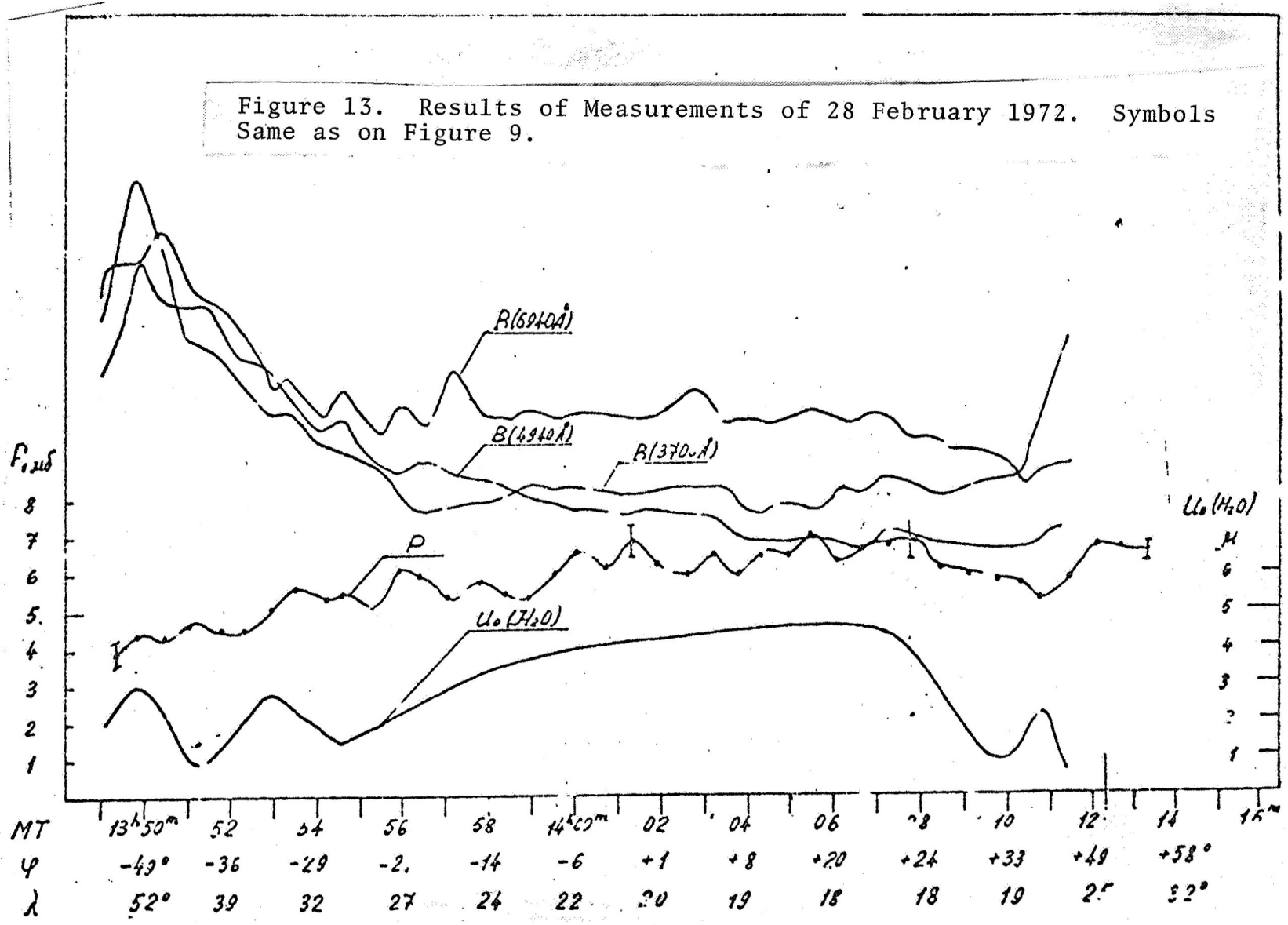

Figure 13. Results of Measurements of 28 February 1972. Symbols Same as on Figure 9.

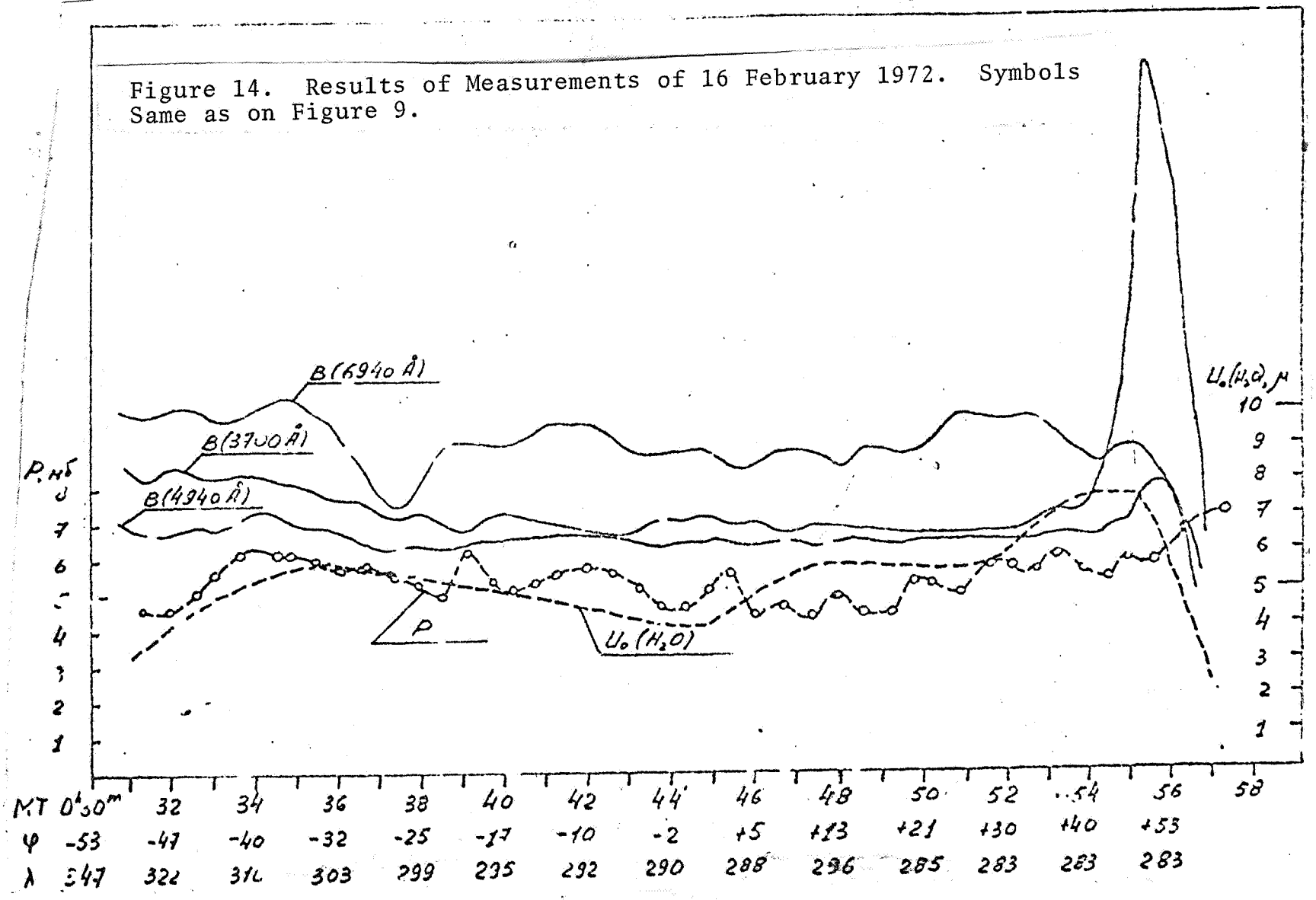

Figure 14. Results of Measurements of 16 February 1972. Symbols Same as on Figure 9.

Dear Reader:

We had to leave this page blank in order to make the following 2-page wide figures spread out right. Therefore, we provide here a little space for any notes you might like to take.

NOTES:

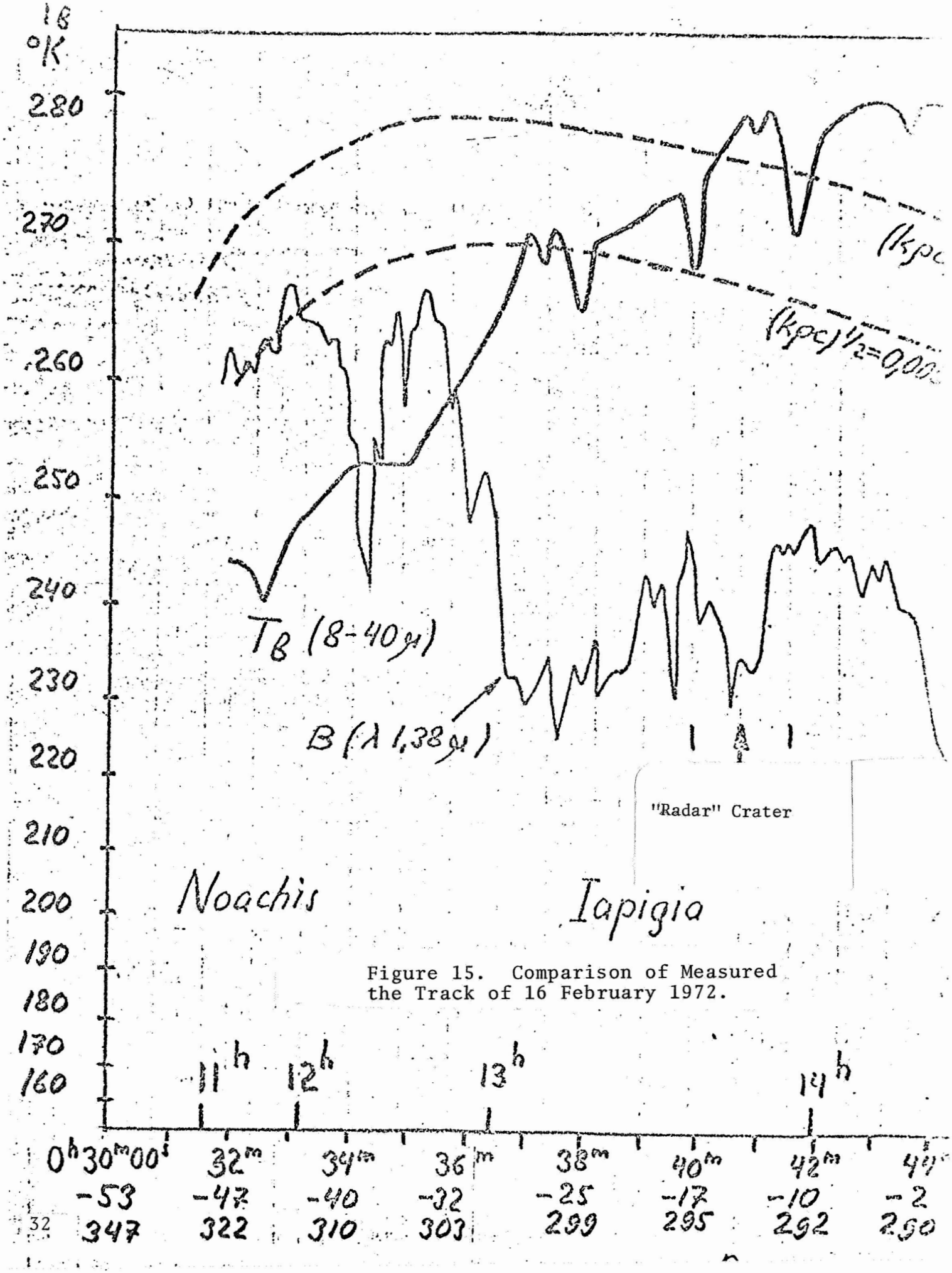

Figure 15. Comparison of Measured the Track of 16 February 1972.

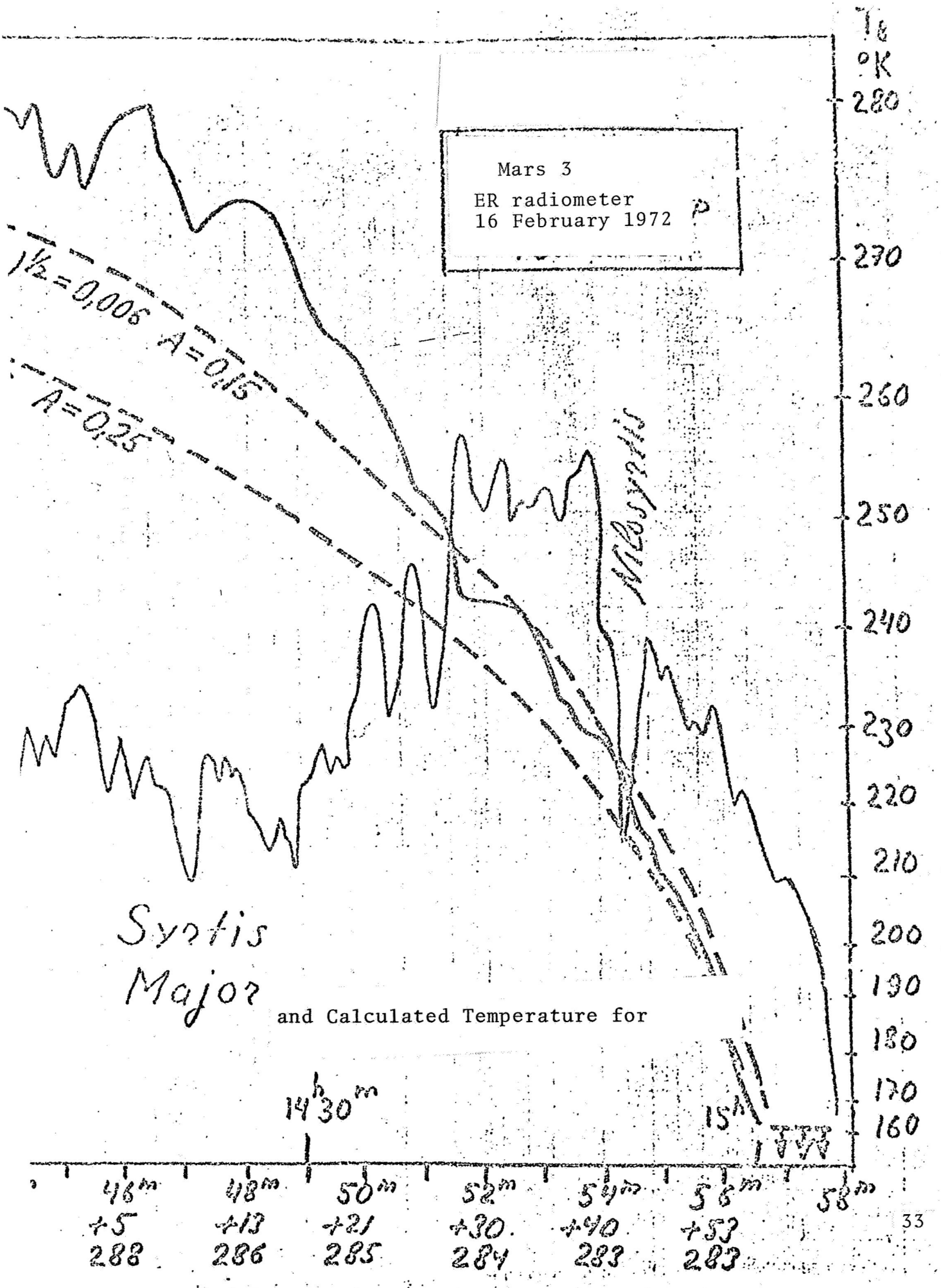
Mars 3
ER radiometer
16 February 1972
$T_{\frac{1}{2}}$=0,005 A=0,15
A=0,25
Mars 3
Syrtis Major
and Calculated Temperature for
$T_б$ °K
280
270
260
250
240
230
220
210
200
190
180
170
160
14h30m
15h
46m 48m 50m 52m 54m 56m 58m
+5 +13 +21 +30 +40 +53
288 286 285 284 283 283

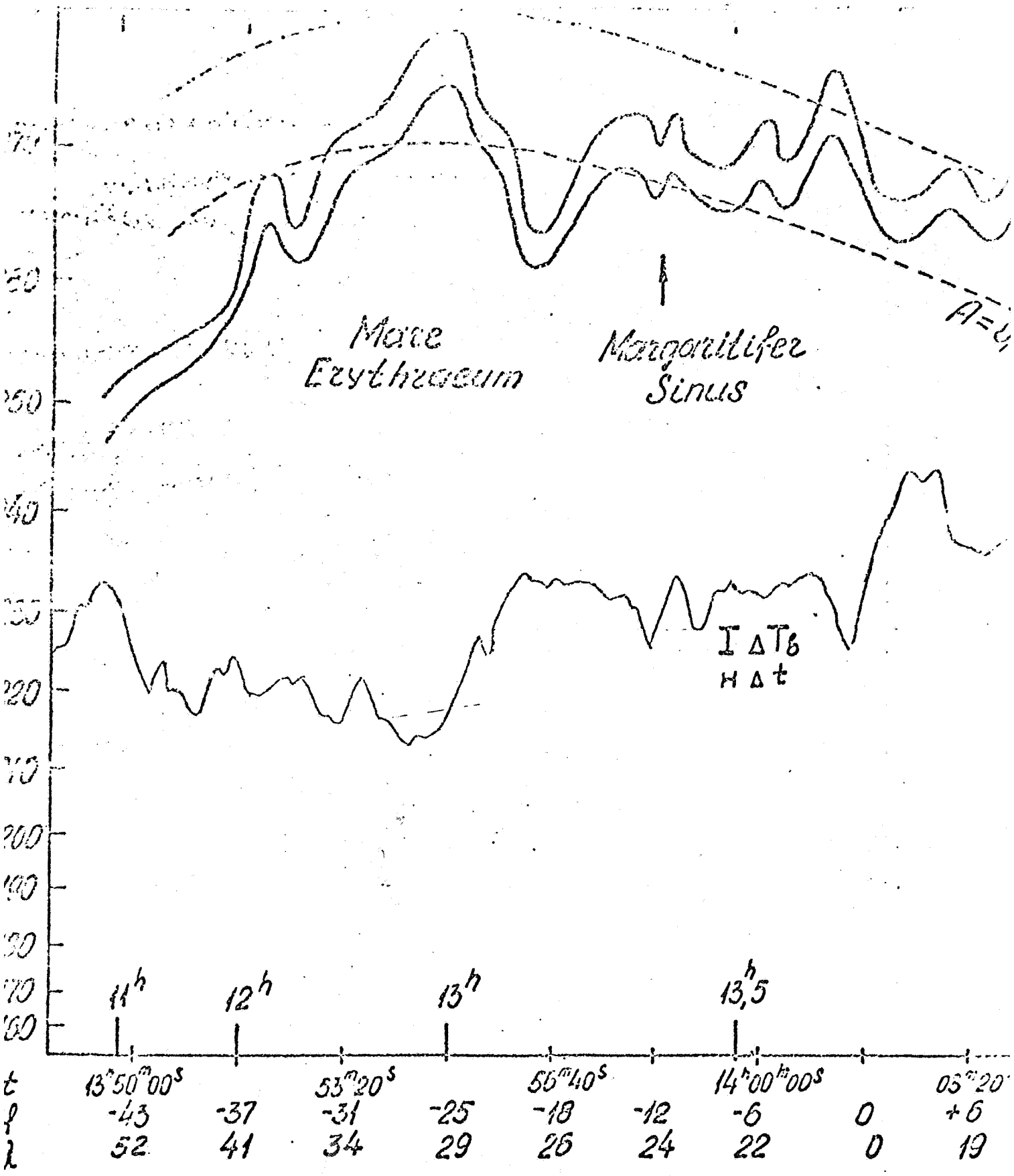

Figure 16. Comparison of Measured
the Track of 28 February 1972.

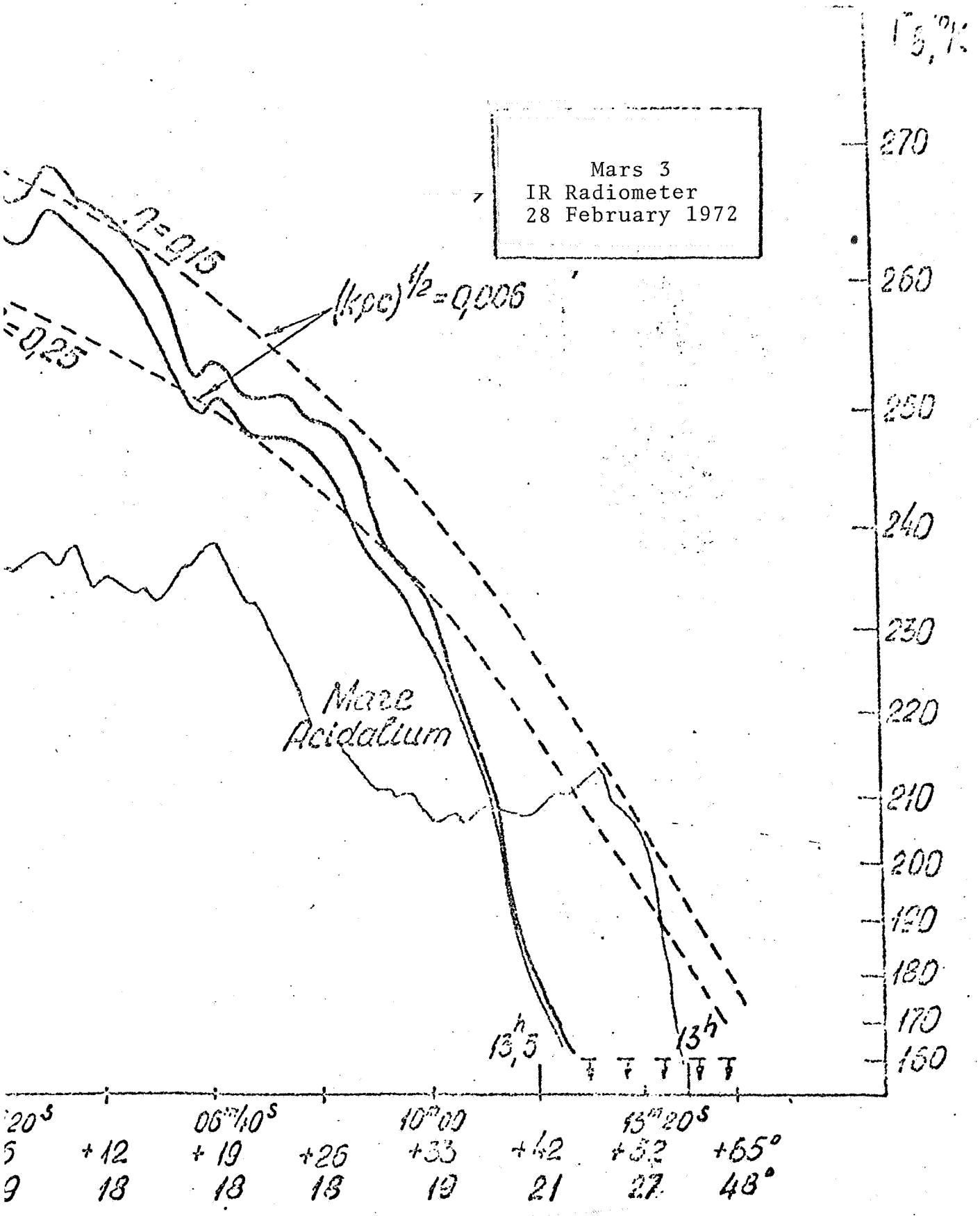

and Calculated Temperature for

TABLE 1

Basic Characteristics of Instruments

Instrument	Purpose	Field of Vision[X], km	Wave-Length, μ	Band Width, μ	Range of Measurements	Internal Accuracy	Accuracy of Absolute Calibration
Infrared Radiometer	Measurement of brightness temperature of surface T_B	30	8-40	∿30	150-300°K	±2° at 250°K ±10° at 160°K	±5° at 250°K ±10° at 160°K
Radio Telescope	Measurement of soil temperature T_{ss} and dielectric constant ε	100	3.4 cm		< 300°K	±20% of T_{ss} 10-50% of ε	
CO_2 Photometer	Measurement of ratios of pressures P and difference of altitudes z based on intensity of CO_2 bands	15	2.014 2.050 2.067 2.075 2.25	0.02 0.02 0.02 0.02 0.02	1 - 50 mb ±20 km	±0.3 + 1.0 mb of P ±0.5 + 2 km of ?	
H_2O Photometer	Measurement of content of H_2O in atmosphere (?) and brightness in continuous spectrum around H_2O band (1.38 μ)	7.5	1.38	0.006	0.5 - 100 μ precipitated water $2\text{-}1200 \cdot 10^{-5}$ W cm^{-2} μ^{-1} $ster^{-1}$	±0.5±2μ $\pm 2 \cdot 10^{-5}$ W $cm^{-2}\mu^{-1}ster^{-1}$	Factor 2^{XX} ±2%
Photometer for 3700-6940 A	Measurement of brightness (B?) in selected narrow sectors of continuous spectrum	45	0.37 0.416 0.494 0.562 0.694	0.03 0.006 0.005 0.007 0.011	$0.1\text{-}2000 \cdot 10^{-5}$ W $cm^{-2}\mu^{-1}ster^{-1}$	±10%[XXX]	±20%

(Footnotes on following page.)

Footnotes to Table 1.

x. Corresponds to width of radiation pattern at 0.5 level, range 1500 km, and zero zenith angle of orbital apparatus. Measurements were performed for visual range CO_2 photometer at intervals of 36 sec (140 km at pericenter) and averaged for 12 sec interval (about 50 km). In other cases, continuous profiles were recorded.

xx. Absolute calibration for H_2O is to be refined by additional laboratory measurements.

xxx. Greater errors may occur due to nonlinearity of scale (logarithmic photometer).

REFERENCES

1. Moroz, V. I., L. V. Ksanfomaliti, Vestnik AN SSSR, No. 9, 1972.
2. Moroz, V. I., L. V. Ksanfomaliti, Icarus, No. 17, p. 408, 1972.
3. Moroz, V. I., L. V. Ksanfomaliti, A. M. Kasatkin et al., Doklady AN SSSR, No. 2, p. 208, 1973.
4. Basharinov, A. E., I. B. Drozdovskaya, S. T. Egorov et al., Icarus, No. 17, p. 540, 1972.
5. Moroz, V. I., L. V. Ksanfomaliti, B. S. Kunashev, et al., Doklady AN SSSR, No. 5, p. 208, 1973.
6. Moroz, V. I., L. V. Ksanfomaliti, A. M. Kasatkin, A. E. Nadzhip, Kosmicheskiye Issledovaniya, No. 6, p. 9, 1972.
7. Moroz, V. I., A. E. Nadzhip, A. B. Gil'barg, Doklady AN SSSR, No. 4, p. 208, 1973.
8. Kolosov, M. A., O. I. Yakovlev, Yu. M. Kruglov, et al., Doklady AN SSSR, 206, 1071, 1972.
9. Ksanfomaliti, L. V., Pribory i Tekhnika Eksperimenta, No. 4, p. 192, 1972.
10. Hanel, R., B. Conreth, W. Hovis et al., Icarus, 17, 423, 1972.
11. Hord, C. W., C. A. Barth, A. I. Stewart and A. L. Lane, Icarus, 17, 443, 1972.
12. Hovis, W. A., W. R. Callahan, JOSA, 56, 639, 1956.
13. Chase, S. C., Jr. Hatsenbeler, H. H. Kieffer et al., Science, 175, 305, 1972.
14. Liberman, A. A., V. I. Moroz, G. S. Khromov, Astron. Tsirk., No. 705, 5 June 1972.
15. Cliore, A., D. L. Canne, G. Fjeldbo et al., Icarus, 17, 484, 1972.
16. Tull, R. G., E. S. Barker, Bull. Am. Astron. Soc., 4, No. 3, p. 11, 1972.
17. Moroz, V. I., O. G. Taranova, Astron. Tsirk., No. 697, 10 May 1972.
18. Parkinson, T. D., D. M. Hunten, Science, 175, 323, 1972.
19. Pang, K., C. W. Hold, Mariner-9 Ultraviolet Experiment: 1971 Mars Dust Storm, University of Colorado, 1972.
20. Leovy, C. B., G. A. Briggs, A. T. Young et al., Icarus, 17, 38, 1972.
21. Ginzburg, A. S., Doklady AN SSSR, 208, No. 3, 1973.